Available online at www.sciencedirect.com

ScienceDirect

Mendeleev Commun., 2017, **27**, 387–389

Mendeleev Communications

Interaction of chemical processes over Pt wire and reactive flows of flame penetration through obstacles in the presence of iron nanopowder

Michail I. Alymov,[a] Nikolai M. Rubtsov,*[a] Victor I. Chernysh,[a] Georgii I. Tsvetkov[a] and Kirill Ya. Troshin[b]

[a] *Institute of Structural Macrokinetics and Materials Science, Russian Academy of Sciences, 142432 Chernogolovka, Moscow Region, Russian Federation. Fax: +7 495 962 8025; e-mail: nmrubtss@mail.ru*

[b] *N. N. Semenov Institute of Chemical Physics, Russian Academy of Sciences, 119991 Moscow, Russian Federation*

DOI: 10.1016/j.mencom.2017.07.023

It has been shown that under certain conditions Pt catalyst can suppress developing flame propagation of methane–oxygen mixtures due to high efficiency of the chain termination by Pt surface coated with Pt oxide layer. Therefore, kinetic factors may be the determining ones even under conditions of high turbulence.

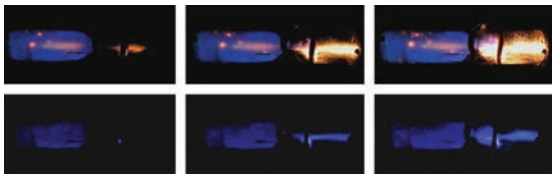

In 1818, Sir Humphrey Davy discovered that methane and oxygen on hot platinum wires could produce a considerable amount of heat in a dark reaction.[1] The interest in the catalytic oxidation process and corresponding reaction systems has been increasing because of the wide potential of this technology in the catalytic combustion processes both in the power generation systems[2–4] and in reduction of the fugitive methane levels;[5] the use of catalytic converters in vehicles permitting to reduce the emission levels of harmful gases.[6,7] The catalytic partial oxidation is also attractive as a processing of intermediate products, which are crucial to synthesize high value products.

The detailed mechanism of methane oxidation in the presence of noble metals has not been well understood yet. Methane chemisorption and methane-deuterium exchange experiments[8] showed that the chemisorption of methane on noble metals involves dissociation into adsorbed methyl or methylene radicals, whose subsequent interaction with the adsorbed oxygen was proposed to lead to either direct oxidation to carbon dioxide and water or the formation of chemisorbed formaldehyde.[9] Up to now, the nature and oxidation states of the reactive surface are largely uncertain and different from one study to another. By the example of palladium, the oxidation may occur on the Pd metal, on a palladium(II) oxide surface, or even on a surface only partially covered with oxygen. Indeed, all three types of catalytic reactions may occur simultaneously. According to X-ray photoelectron spectroscopy (XPS) measurements,[10] the smaller the size of the palladium crystallites, the greater its tendency to form the oxide. Some other uncertainties of the catalytic oxidation of methane are the role of the catalyst support, the effect of particle size and the choice of the catalyst precursor salt.

Note that the kinetics of the catalytic combustion is only relevant in the area where the intrinsic surface reaction is the key process. In addition, the reaction finally reaches a point where a large amount of thermal energy is released (as a result of complete consumption of the reactant), which may result in a significant temperature increase, thus the stability of the catalyst at high operating temperatures is of great importance in the performance of the catalytic system.[2] Moreover, noble metals form oxides and other compounds, which, depending on their reactivity, determine both the rate and the mechanism of catalytic process; this fact noticeably complicates the search for optimum catalysis conditions. For instance, Pd easily transforms into PdO at temperatures lower than 1100 K, whereas PtO_2 is unlikely to be generated below 825 K and it is a very unstable compound. Due to the greater stability of PdO in comparison with PtO_2, in the case of Pd-based catalyst the active phase is PdO; while in the case of Pt-based catalyst the active phase is metallic Pt. The activity of PdO is greater than that of Pt, which results in higher conversions in the presence of PdO.

The reaction temperature significantly affects the level of the catalyst activity *via* two ways. The first one is an apparent shift in the activation energy of methane combustion over Pd catalyst as the temperature increases. The latter was reported to be a function of catalyst composition.[11] Although it is crucial to differentiate changes in apparent activation energy occurring as a result of the onset of mass and heat transfer effects, indeed, the literature data evidence that there is a genuine activation energy shift in the reaction of methane combustion over Pd catalyst. Thus, for methane combustion over noble metal catalysts in the temperature range of 500–800 K, a sharp change in the values of reaction activation energy was observed.[9]

Therefore, the emergence and participation of chemically active surface in gas combustion (for example, H_2 combustion over Pt surface) significantly complicate the understanding of the process due to the occurrence of a number of new key parameters. These include the dependence of the catalyst activity on its chemical composition, temperature and conditions of mass transfer.

This work was aimed at the investigation of the role of Pt in the flame propagation in the methane oxidation under conditions of turbulent flow.[†] As it was considered previously,[12] surface reactions over Pt surface are mainly highly activated ($\geqslant$ 20 kcal mol^{-1}). Therefore, one can expect not only inert behavior of Pt catalyst at comparably low temperatures, at which the catalyst does not have time to be heated, but also suppression of the process due to the complex mechanism of heterogeneous termination of atoms and radicals on the Pt surface.

Four types of single flat obstacles were used: (1) with an opening of 25 mm in diameter closed with a flat iron net (wire d = 0.1 mm, cell size of 0.15 mm^2); (2) the same one with a turn of

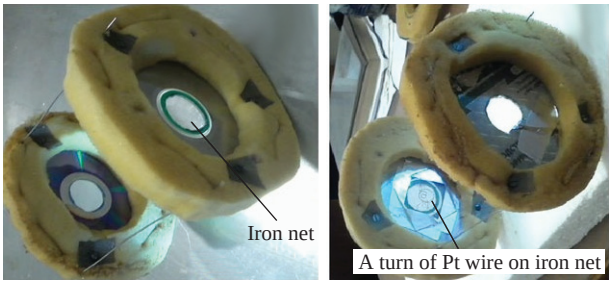

Figure 1 Complex obstacles (3) and (4).

Pt wire 0.2 mm in diameter attached to the net; (3) with an opening of 25 mm in diameter and the obstacle (1) (Figure 1); (4) the same one and the obstacle (2) (Figure 1). Evidently, obstacles (3) and (4), which contain two consecutive obstacles, are more effective turbulence stimulators than obstacles (1) and (2).

The typical sequences of frames of high-speed video of the flame front (FF) propagation through the obstacles (1) and (2) are shown in Figure 2. In accordance with Figure 2(*a*), the flame of the combustible mixture penetrates through the obstacle without Pt wire twice as fast as through the obstacle equipped with a Pt wire. It means that Pt under our experimental conditions has a noticeable suppressing influence on flame propagation even in the turbulent flow. Figure 3 also demonstrates that the flame penetrates faster through the complex obstacle without Pt wire than through that equipped with a Pt wire. However, the

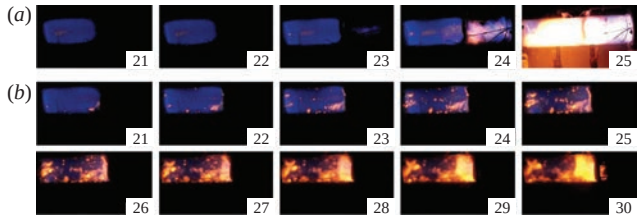

Figure 2 High-speed video frames of FF propagation through (*a*) obstacle (1) and (*b*) obstacle (2). Initial pressure 170 Torr. The frame numbers after discharge are indicated.

† Flame propagation in stoichiometric mixtures of methane with oxygen diluted with CO_2 or Kr at initial pressures in the range of 100–200 Torr and 298 K was investigated in the pumped out horizontally located cylindrical quartz reactor of 70 cm in length and of 14 cm in diameter. The reactor with blunt ends was fixed in two stainless steel frames, supplied with inlets for gas, system of gas injection and a safety shutter, which swung outward when the total pressure in the reactor exceeded 1 atm. The obstacles with empty openings were placed first, *i.e.* initially the flame reached the empty opening. The second obstacle was placed at the distance of the 'flame jump'[13] from the first one. This distance was 12 cm in our experiments. A pair of spark ignition electrodes was located near the left blunt end of the reactor.[13,14] The reactor was filled with the mixture up to necessary pressure. Then, spark initiation was performed (the discharge energy was 1.5 J). Filming of high speed video of ignition dynamics and flame front (FF) propagation was performed from the side of the reactor[13,14] by a Casio Exilim F1 Pro color high-speed digital camera (frame frequency of 600 s^{-1}). Simultaneous detection of radicals CH ($A^1\Delta$–$X^2\Pi$) at 431 nm[15] was carried out by two high-speed movie cameras Casio Exilim F1 Pro, one of which was equipped with a 430 nm interference filter. The video file was stored in computer memory and its time-lapse processing was performed. The reagents were of chemically pure grade. The combustible mixture (15.4% CH_4 + 30.8% O_2 + 46% CO_2 + 7.8% Kr) was prepared prior to experiment; CO_2 was added to enhance the quality of filming by decreasing the FF propagation rate; Kr was added to diminish the discharge threshold. In a number of experiments the flat obstacle 14 cm in diameter with a single opening of 25 mm in diameter was provided with a reservoir where iron nanopowder was placed (Figure 1).[14]

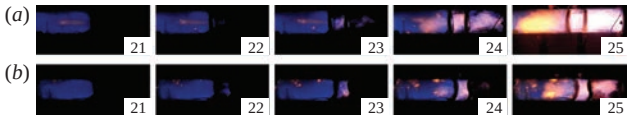

Figure 3 High-speed video frames of FF propagation through (*a*) obstacle (3) and (*b*) obstacle (4). Initial pressure 170 Torr. The frame numbers after discharge are indicated.

suppressing influence of Pt under conditions of higher turbulence is less pronounced as compared with Figure 2(*b*).

To estimate the contribution of chemical factors, the emission of CH radicals ($A^1\Delta$–$X^2\Pi$) at 431 nm and the emission over the whole spectral interval in the presence of Fe nanopowder were recorded simultaneously. Iron nanoparticles,‡ which were blown out of the reservoir through an opening with a gas flow into the flame, were ignited in a methane flame. Thus, burning iron nanoparticles visualized the gas flow during combustion. In case of the complex obstacle (3) in the absence of the Pt wire (Figure 4), Fe nanopowder ignites inside the FF, so the gas flow is visualized only when the flame front reaches the obstacle. Meanwhile, the illumination by a laser sheet allows one to detect the flow from the very beginning of the process.[14] It is also seen that the mesh on the second obstacle does not obstruct the movement of iron nanoparticles. It is important that the intensity of emission of CH radicals monotonically increases after the flame reaches the obstacle.

The main difference in the process of flame penetration through the complex obstacle (4) in the presence of the Pt wire (Figure 5) from that shown in Figure 4 is that the emission of CH radicals practically passes off (frame 25); the combustible mixture ignites again at the blunt end of the reactor just as in the absence of iron nanoparticles [Figure 3(*b*)].

It means that even the presence of burning Fe nanoparticles does not visibly influence the process of methane flame penetration; however, a Pt wire on the obstacle affects the process both in the presence and in the absence of nanoparticles. As shown in

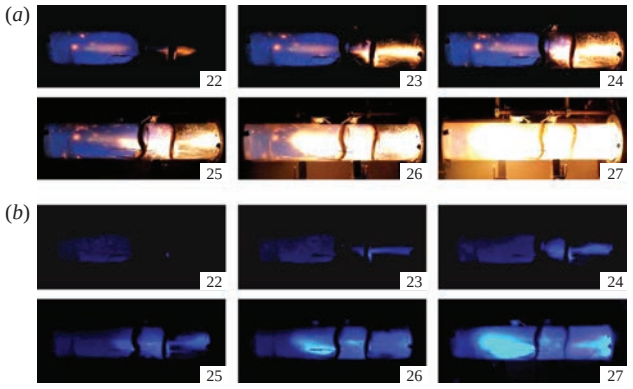

Figure 4 High-speed video frames of FF propagation through obstacle (3): (*a*) without and (*b*) with interference filter 430 nm placed before the camera. Initial pressure 170 Torr. The frame numbers after discharge are indicated.

‡ Iron nanopowders were obtained by the method of chemical metallurgy, whose main stages were synthesis of the hydroxides of metals by means of alkali treatment of metal salts, sedimentation and drying of the hydroxides, their reduction and passivation.[16] Iron hydroxide was synthesized by the heterophase interaction of solid iron salt with the solutions containing hydroxyl groups under suppression of dissolution of solid salt by the reaction between $FeCl_3$ and NH_4OH. After sedimentation of iron hydroxide it was washed in a Buchner funnel to pH 7 and dried on air until dust was formed. The reactor[17] with a sample of 1 mm thick iron hydroxide powder layer was incubated in the furnace at 400 °C for 1 h in hydrogen flow; then it was cooled to 20 °C in argon flow. For passivation of the iron nanopowder, which was performed in the same reactor, 0.6% of O_2 was added to argon stream at 20 °C.

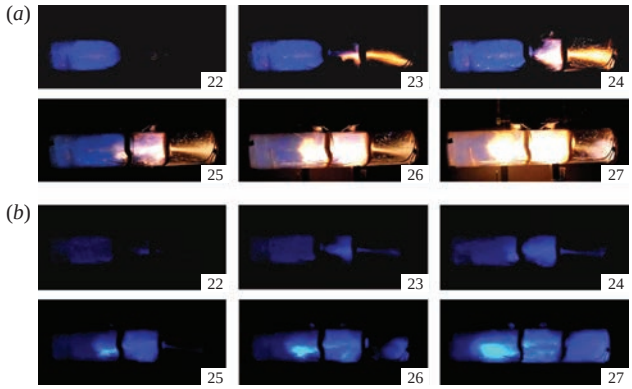

Figure 5 High-speed video frames of FF propagation through obstacle (4): (*a*) without and (*b*) with interference filter 430 nm placed before the camera. Initial pressure 170 Torr. The frame numbers after discharge are indicated.

Figure 5(*b*), Pt provides a strong decrease in the intensity of emission of CH radicals, *i.e.* one can assume the high rate of chain termination over the Pt surface in agreement with ref. 18. In addition, Pt wire is coated with a thick surface layer of Pt oxide which exhibits other properties than pure Pt.[19] The flame penetrates through the Pt containing obstacle, apparently if Pt is heated enough [see Figure 2(*b*)], though the heat balance on the Pt surface in a reactive turbulent flow is rather difficult to calculate. We approximately estimated the contribution of chemical factors (chain termination on the obstacle surface) by numerical modeling on the basis of compressible dimensionless reactive Navier–Stokes equations in low Mach number approximation,[14,20] which describes flame propagation in a two-dimensional channel. The equations showed a qualitative consent with experiments.[13,14] The problem was solved by finite element analysis (FlexPDE 6.08 package[21]). The simple chain mechanism[14] was used. Initiation condition was taken as $T = 10$ on the right boundary of the channel; there was a complex orifice in the channel. Boundary conditions (including the orifice) were $C_\xi = 0$, $u = 0$, $v = 0$, $\rho_\xi = 0$, $n_\xi = 0$ [Figure 6(*a*)] or $n = 0$ only on the plain mesh surface [Figure 6(*b*), the second obstacle from the right], as well as a convective heat exchange $T_t = T - T_0$, where ξ is the dimensionless coordinate. The results of calculations (Figure 6) show that the intensive termination of active intermediate on the

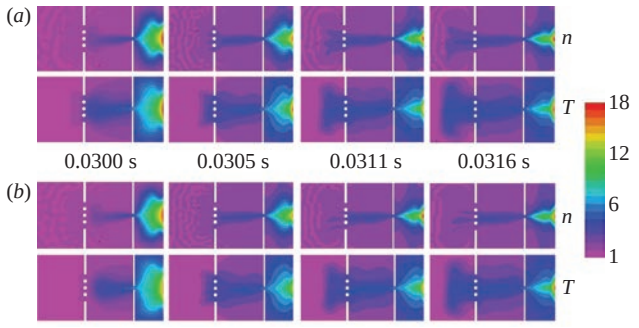

Figure 6 Results of calculation of the process of flame propagation through the complex orifice. Change in dimensionless concentration of active intermediate n and temperature T for flame propagation through a complex opening for (*a*) $n_\xi = 0$ on the mesh (type II of boundary conditions) and (*b*) $n = 0$ on the mesh (type I of boundary conditions). The scale of dimensionless temperature is presented on the right.

mesh surface ($n = 0$) markedly influences the flame penetration, namely, causes the marked delay in flame penetration through the mesh in comparison with the case of $n_\xi = 0$. Hence, regardless of the qualitative consideration, as well as a rather conventional modeling of the plain mesh, we managed to take into account the efficient action of the active surface on the features of the flame penetration.

In conclusion, a Pt catalyst may suppress combustion under certain conditions and thereby shows the opposite effect due to the high efficiency of Pt surface coated with a Pt oxide layer in the reaction of chain termination. Therefore, kinetic factors may be the determining ones even under conditions of high turbulence.

We are grateful to V. A. Zelensky (Institute of Structural Macrokinetics and Materials Science, RAS) and A. B. Ankudinov (Institute of Metallurgy and Materials Science, RAS) for granting a sample of iron nanopowder.

This work was supported by the Russian Science Foundation (project no. 16-13-00013).

References

1 H. Davy, *Philos. Trans. R. Soc. London, Ser. A*, 1817, **107**, 77.
2 J. H. Lee and D. L. Trimm, *Fuel Process. Technol.*, 1995, **42**, 339.
3 O. Deutschmann, L. I. Maier, U. Riedel, A. H. Stroemman and R. W. Dibble, *Catal. Today*, 2000, **59**, 141.
4 M. Lyubovsky, H. Karim, P. Menacherry, S. Boorse, R. LaPierre, W. C. Pfefferle and S. Roychoudhury, *Catal. Today*, 2003, **83**, 183.
5 S. Salomons, R. E. Hayes, M. Poirier and H. Sapoundjiev, *Catal. Today*, 2003, **83**, 59.
6 J. K. Lampert, M. S. Kazia and R. J. Farrauto, *Appl. Catal., B*, 1997, **14**, 211.
7 P. Gélin and M. Primet, *Appl. Catal., B*, 2002, **39**, 1.
8 A. Frennet, *Catal. Rev. Sci. Eng.*, 1974, **10**, 37.
9 C. F. Cullis and B. M. Willatt, *J. Catal.*, 1983, **83**, 267.
10 R. F. Hicks, H. Qi, M. L. Young and R. G. Lee, *J. Catal.*, 1990, **122**, 280.
11 R. E. Hayes, S. T. Kolaczkowski, P. K. C. Li and S. Awdry, *Chem. Eng. Sci.*, 2001, **56**, 4815.
12 X. Zheng, J. Mantzaras and R. Bombach, *Proc. Combust. Inst.*, 2013, **34**, 2279.
13 N. M. Rubtsov, I. M. Naboko, B. S. Seplyarskii, V. I. Chernysh, G. I. Tsvetkov and K. Ya. Troshin, *Mendeleev Commun.*, 2016, **26**, 61.
14 N. M. Rubtsov, V. I. Chernysh, G. I. Tsvetkov and K. Ya. Troshin, *Mendeleev Commun.*, 2017, **27**, 101.
15 B. Lewis and G. von Elbe, *Combustion, Flames and Explosions of Gases*, 3rd edn., Academic Press, New York, 1987.
16 V. A. Zelensky, M. I. Alymov, A. B. Ankudinov and I. V. Tregubova, *Perspektivnye Materialy*, 2009, no. 6, 83 (in Russian).
17 M. I. Alymov, N. M. Rubtsov, B. S. Seplyarskii, V. A. Zelensky and A. B. Ankudinov, *Mendeleev Commun.*, 2016, **26**, 452.
18 G. I. Golodets and V. M. Vorotyntsev, *React. Kinet. Catal. Lett.*, 1984, **25**, 75.
19 N. M. Rubtsov, A. N. Vinogradov, A. P. Kalinin, A. I. Rodionov, K. Ya. Troshin, G. I. Tsvetkov and V. I. Chernysh, *Mendeleev Commun.*, 2016, **26**, 160.
20 A. Majda, *Equations for Low Mach Number Combustion*, Center for Pure and Applied Mathematics, University of California, Berkeley, 1982, PAM-112.
21 G. Backstrom, *Simple Fields of Physics by Finite Element Analysis*, GB Publishing, Malmo, 2005.

Received: 31st August 2016; Com. 16/5035